Kinetic–transport models and the design of catalysts and reactors for the oxidative coupling of methane

Sebastian C. Reyes, C.P. Kelkar and Enrique Iglesia [1]

Corporate Research Laboratories, Exxon Research and Engineering Company, Route 22 East, Annandale, NJ 08801, USA

Received 26 January 1993; accepted 30 March 1993

The design of catalytic pellets and reactors using detailed kinetic–transport models is illustrated for the oxidative coupling of methane to form ethane and ethylene. Oxygen sieving within diffusion-limited pellets and staged oxygen injection reactors increase C_2 selectivity by inhibiting full oxidation homogeneous pathways that lead to CO and CO_2 products. Our simulations suggest that high densities of surface sites with kinetics that depend weakly on oxygen concentration are required to benefit from oxygen-sieving catalyst and reactor schemes. These sites favor beneficial surface activation processes even at the low oxygen concentrations present within staged injection reactors and diffusion-limited pellets. Controlled introduction of stoichiometric oxygen reactants leads to C_2 yields as high as 50%; the reactions, however, occur at much slower rates and require much greater reactor volumes than in conventional cofeed reactors.

Keywords: Reaction–transport; catalyst design; reactor design; methane coupling

1. Introduction

Oxidative coupling of methane is a potentially attractive route for the direct conversion of methane to C_2 hydrocarbons [1]. Industrial practice of this technology will require catalyst and reactor designs that increase ethylene yields above presently attainable values (about 20–25%). Our work explores such improved designs by using mechanistic reaction–transport models of homogeneous–heterogeneous methane conversion pathways.

Oxidative coupling proceeds via a bimodal scheme that includes radical generation at surfaces and coupling and oxidation reactions of these radicals in the surrounding gas phase [2–4]. In general, C_2 selectivity decreases with increasing methane conversion, leading to maximum yields of C_2 products at intermediate levels of conversion. This selectivity loss, and the ultimate decrease in C_2 yields at

[1] Present address: Department of Chemical Engineering, University of California at Berkeley, Berkeley, CA 94720, USA.

high methane conversion, is characteristic of reaction sequences where intermediate products (C_2H_4, C_2H_6) are more reactive than reactants (CH_4).

2. Methods

Our coupled reaction–transport models include detailed descriptions of kinetic, diffusion, and convection processes within porous catalyst pellets held in packed-bed reactors. These models incorporate surface and gas phase reaction networks [5,6], and improved structural models of mesoporous solids [7] into mass balance equations within catalyst pellets and plug-flow reactors. Model simulations describe how catalyst structural properties (porosity, pore diameter, pellet size, site density), site chemistry (turnover rate, selectivity, kinetic orders), and reactor design (staged injection or membrane reactors) affect maximum attainable C_2 yields (defined as the product of C_2 selectivity and fractional CH_4 conversion).

Our models extend previous approaches by combining detailed descriptions of homogeneous and surface kinetics with convective and diffusive transport processes. Our simulations examine the effect of critical design parameters, such as catalyst structural properties, kinetic response to reactant and product concentrations, and reactor configurations on the maximum attainable yields of desired C_2 products. These models guide the design of conceptual catalysts and reactors for optimum yields. Below, we describe the general features of the models; additional details are reported elsewhere [5,6].

2.1. HOMOGENEOUS REACTION NETWORK

The homogeneous kinetic model was assembled from available kinetics of thermal reactions of hydrocarbons in the presence of oxygen [8–13]. It includes 145 reactions and 28 reactive species; mass action kinetics are used to describe most reaction steps but processes controlled by collisional activation and energy relaxation are also rigorously described [5]. Reverse reaction rates are included for all steps; they were assembled from reported kinetics, when available, or obtained from thermodynamic data for the overall elementary step. The resulting homogeneous kinetic model accurately describes experimental data at 900–1300 K and 0–10 MPa without any adjustable parameters.

Our homogeneous kinetic model shares its common origins in the literature of free-radical processes with several others recently reported [14–17]. Our model differs from previous ones in the specific choice of chemical reactions and reactive species from the large manifold of available kinetic data. Its merit lies in its ability to describe experimental data in homogeneous reactors without adjusting any kinetic rate constants and in its reasonable scope, which preserves important chemical steps but limits them to a number that can be handled efficiently within our computationally-intensive reaction–diffusion models.

2.2. SURFACE REACTION NETWORK

The wide range of catalytic materials and of empirical kinetic equations reported in the literature [2,3], and the difficulty in decoupling surface and homogeneous kinetics within experimental results, led us to use general kinetic expressions to describe the heterogeneous generation rate of methyl,

$$CH_4 + \tfrac{1}{4}O_2 = \cdot CH_3 + \tfrac{1}{2}H_2O\,, \tag{1}$$

$$R_i = k_i[CH_4][O_2]^n\,,$$

and ethyl radicals,

$$C_2H_6 + \tfrac{1}{4}O_2 = \cdot C_2H_5 + \tfrac{1}{2}H_2O\,, \tag{2}$$

$$R_j = k_j[C_2H_6][O_2]^n\,.$$

Both rates were assumed to depend linearly on hydrocarbon concentration but the dependence on oxygen concentration (n) was allowed to vary between 0 and 1 in our simulations. The form of these kinetic expressions is consistent with those obtained from the only reliable direct measurements of surface-catalyzed methyl radical formation rates on metal oxides [18,19]. Our intent is not to describe the behavior of specific catalysts; thus, we consider k_i, k_j, and n adjustable parameters that can be varied in the design of optimum catalytic materials.

In our simulations, we assume a hypothetical surface capable of activating C–H bonds in methane and ethane with the above described kinetics, but which does not catalyze complete combustion of these species to CO_x; in other words, CO_x is formed exclusively in gas phase reactions of reactants and products. In this manner, we explore the maximum yields achievable on selective catalysts; several catalysts give very high initial C_2 selectivities at low methane conversions [2–4,20], suggesting that *catalytic* methane (and ethane) combustion is slow at oxidative coupling conditions at least on some catalytic materials.

Volumetric reaction rates (R_i, molecules $m^{-3}\,s^{-1}$)

$$R_i = 10^6 SdN\Theta \tag{3}$$

are determined by textural and intrinsic chemical properties of the catalytic surface, such as surface area (S, m^2/g), particle density (d, g/cm^3), site density (Θ, sites/m^2), and site reactivity (N, turnover rate, molecules/site s). Some of these structural catalyst properties also control mass transport rates within catalyst pellets [5–7]. Here, we have selected typical values of S (10 m^2/g), d (2 g/cm^3), and Θ (10^{19} sites/m^2) in order to restrict our discussion to the effects of site reactivity (N) and selectivity (g) on C_2 yields. Site selectivity (g) is defined as the ratio of the ethane (k_j, in (2)) to methane (k_i, in (1)) surface activation rate constants. These assumptions lead to a simple model of surface reactions described by the parameters n, g, and N; the effect of these parameters on C_2 yields is examined in section 3.

2.3. KINETIC–TRANSPORT MODEL OF CATALYTIC PELLETS AND REACTORS

Our models describe the coupling among reactive and diffusive processes within pellets and convection and reaction processes occurring within interstitial reactor voids [5]. The resulting equations describe radial concentration gradients within catalyst pellets and axial concentration gradients along isothermal plug-flow reactors. Mass balance and diffusion equations for all 28 chemical species involved in 145 reversible reaction steps are included in our simulations. We do not account for temperature gradients in our model; they can be incorporated by the simple inclusion of an overall energy balance in the model equations. Modest temperature gradients (<200 K) do not significantly influence C_2 selectivity or maximum C_2 yields in oxidative coupling reactions.

The resulting system of coupled ordinary differential equations and boundary value problems is solved numerically [5]. We use this general model to study three types of catalyst–reactor systems: homogeneous reactors, bimodal (heterogeneous–homogeneous) reactors without intrapellet concentration gradients, and bimodal reactions within transport-limited pellets. We also examine the effects of controlled introduction of the oxygen reactant along the catalyst bed and of oxidative coupling membrane reactors.

3. Results and discussion

3.1. HOMOGENEOUS REACTORS

Homogeneous reactor simulations are compared with experimental data obtained using empty reactors in fig. 1. The model predictions are consistent with experimental C_2 selectivities and with the observed effect of increasing methane

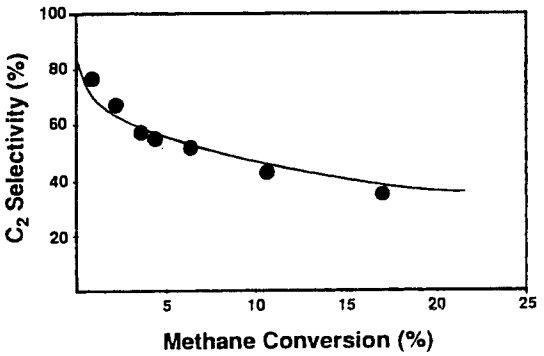

Fig. 1. Oxidative coupling of methane in homogeneous reactors. Simulated and experimental results. (1073 K, 46.7 kPa methane, 23.3 kPa oxygen, experimental points from ref. [20]).

conversion (fig. 1, 1073 K) [21]. Extensive model simulations [5] and experimental results [2,3,20,21] suggest that C_2 yields above 10% and initial C_2 selectivities (at $<5\%$ conversion) greater than 80% cannot be achieved using homogeneous reactors because of competing homogeneous oxidation of methane reactants and of ethane and ethylene products to CO.

The introduction of a selective surface function that catalyzes radical formation decouples the activation from the homogeneous combustion steps by providing a source of methyl radicals that does not catalyze oxidation steps. These surface sites lead to an increase in the steady-state concentration of gas phase methyl radicals, conditions that favor their bimolecular coupling to form ethane.

3.2. BIMODAL HOMOGENEOUS–HETEROGENEOUS REACTORS

The presence of more active catalytic sites fully accessible to reactants (i.e., unaffected by intrapellet transport restrictions) leads to higher C_2 selectivities and yields (fig. 2). Methyl radical coupling steps benefit from heterogeneous radical generation to a greater extent than homogeneous oxidation pathways. C_2 yields increase because of the second-order dependence of coupling steps on methyl radical concentration, compared with the near first-order dependence for the secondary oxidation of C_2 products to CO_x suggested by our homogeneous kinetic network.

Curve A (fig. 2) describes the effect of a selective catalytic surface that converts methane but not ethane or ethylene to the corresponding alkyl radical ($g = 0$). We also assume that surface sites do not catalyze combustion of methane or C_2 products to CO_2. Turnover rates lower than 0.1 s^{-1} do not increase C_2 yields because homogeneous radical generation remains the predominant source of methyl radicals. C_2 yields as high as 50% can be achieved with very active catalysts; they will

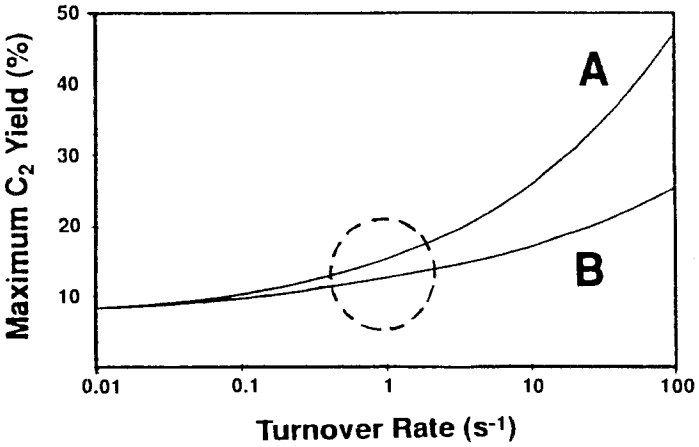

Fig. 2. Simulated effect of site turnover rate (N) on maximum C_2 yields (A: $g = 0$; B: $g = 4$). (1073 K, 67 kPa methane, 33 kPa oxygen.)

require, however, site densities above 10^{19} m^{-2} and turnover rates greater than 100 s^{-1}, values much greater than presently available (see dashed region in fig. 2). These high volumetric activities often introduce severe diffusional restrictions in conventional reactors with concomitant losses in selectivity and poor catalyst utilization (see section 3.5).

Yields above 50% also require catalysts with high selectivity for methane activation ($g = 0$). Curve B (fig. 2) shows how maximum C_2 yields decrease markedly when catalyst sites also activate ethane molecules with the selectivity expected from the relative strength of C–H bonds in methane and ethane and from their relative thermal activation rates ($g = 4$). In summary, our simulations suggest that C_2 yields above 20% require very high densities ($\gg 10^{19}$ m^{-2}) of very active ($N > 10\ s^{-1}$) and also very selective ($g < 1$) sites.

3.3. STAGED INTRODUCTION OF OXYGEN INTO BIMODAL REACTORS

Bimodal reaction schemes can also benefit from differences in the oxygen kinetic dependence between homogeneous combustion pathways and heterogeneous methyl formation steps. The homogeneous kinetic network confirms that gas phase oxidation of primary C_2 products is near first-order in oxygen concentration. Thus, any heterogeneous radical generation steps with oxygen kinetic orders less than unity will benefit from lower oxygen concentrations within the reactor. The use of methane-rich feeds, however, severely limits the level of methane conversion that can be achieved because the stoichiometric oxygen reactant is rapidly depleted and low oxygen concentrations significantly decrease overall methane activation rates.

A reactor where the oxygen reactant is distributed throughout many injection ports along the axial reactor dimension maintains low oxygen concentrations but still provides the stoichiometric oxygen reactants required to reach high methane conversions. We have simulated this type of reactor by dividing the amount of oxygen normally introduced at the reactor inlet along M injection ports. After each oxygen injection, the oxygen–methane mixture is allowed to react until 85% of the oxygen introduced is converted; then, additional oxygen is added at the next injection port.

Our simulations predict that distributed oxygen injection reactors increase maximum C_2 yields from 14 to 30% as the number of injection points increases from 1 (cofeed) to 1000, for the case of surface sites with first-order oxygen kinetics (Curve A, fig. 3). A large number of injection points (> 100) is required to obtain significant yield improvements because surface activation to form methyl radicals ($n = 1$) and homogeneous C_2 oxidation steps ($n \gtrsim 1$) show similar kinetic responses to oxygen concentration; therefore, selectivity improvements occur only at very low oxygen concentrations. These low concentrations, in turn, lead to extremely slow heterogeneous activation steps and increase the residence time and reactor volume required to achieve maximum C_2 yields by a factor of about 3000 (for 1000

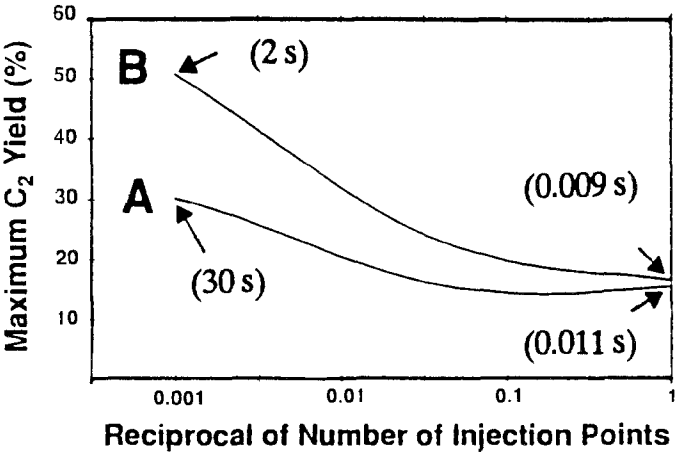

Fig. 3. Simulated effect of staged oxygen injection on maximum C_2 yields (curve A: $N = 1\ s^{-1}$, $g = 0$, $n = 1$; curve B: $N = 1\ s^{-1}$, $g = 0$, $n = 0.5$). (1073 K, 67 kPa methane, 33 kPa oxygen.) (Numbers in parentheses denote residence times.)

injection points) over those required when oxygen and methane are cofed at the reactor inlet (see caption of fig. 3).

The importance of surface kinetics with low oxygen kinetic order ($n < 1$) is also clearly shown by comparing curves A ($n = 1$) and B ($n = 0.5$) in fig. 3. The stronger beneficial effect of oxygen staging on catalysts with half-order oxygen kinetics is consistent with our previous discussion. For plug-flow reactors with 1000 injection points, C_2 yields reach 50% and the required increase in bed residence time and reactor volume is less severe (a factor of about 200) than on sites with first-order oxygen kinetics (fig. 3). Also, controlled oxygen injection begins to affect yields at lower staging intensity ($M = 10$) when sites with half-order oxygen kinetics are used. Ultimately, catalytic sites with zero-order kinetics are best for staged injection reactors. In the limit of low oxygen concentration, however, mass action kinetics, defined by the reaction stoichiometry, always lead to pressure orders greater than zero for any reactant appearing in the stoichiometric equation. Therefore, the search for improved catalytic materials should stress the need for surface methyl radical formation functions with low oxygen kinetic response, a property that would permit their efficient operation at low oxygen concentrations. This task is complicated by the experimental coupling of surface and gas phase kinetics, which requires detailed descriptions of the homogeneous pathways in order to separate the heterogeneous component from the overall kinetic response. The search for these types of oxidative coupling catalysts can greatly benefit from recent advances in the microkinetic modeling of surface reactions [22], where the molecular and chemisorption bond energies of adsorbed intermediates are used to predict the kinetic rate constants of elementary surface steps.

The results of fig. 3 show that a large number of injection points are required to benefit from controlled injection schemes, even on catalysts with low-order

kinetics; this number is significantly larger than those explored in many previous experimental and theoretical studies of staged oxygen injection [23–25]. The latter studies suggest only small benefits of these schemes, consistent with the predictions of our simulations. Clearly, previous investigations have not been carried out within the range of staging intensity ($M > 10$) required to significantly improve C_2 yields.

Choudhary et al. [23] used distributed feed reactors with four injection points and observed a slight increase in C_2 selectivity and yield on La-promoted MgO catalysts. Curiously, the activation rate was higher with distributed feeds, even though the oxygen concentrations and the kinetic driving force were lower and the methane conversion rate actually decreased with increasing methane/oxygen ratio. This observation suggests unusual negative order oxygen kinetics or experimental difficulties in their measurements of the methane conversion in staged reactors.

Santamaria et al. [24] carried out computer simulations of four plug-flow reactors in series with injection points between reactors using a simplified kinetic model with three reactions and four chemical species. Their simulations do not suggest any yield or selectivity improvements when single and distributed feed simulations are compared at similar methane conversion. Smith [25] reports an increase in catalyst productivity when the oxygen component in the feed is introduced at two axial positions in a fixed-bed reactor (973 K, $O_2/CH_4 = 0.5$). C_2 selectivities or yields are not reported and single and distributed feed schemes are compared at different methane and oxygen concentrations, making comparisons difficult. It appears that any productivity improvements obtained in this work reflect the higher average methane partial pressures used in these distributed feed experiments. Our staged-injection simulations (fig. 3) and the weak effects of oxygen concentration on C_2 yields throughout the range studied in this reference (fig. 4) suggest that the

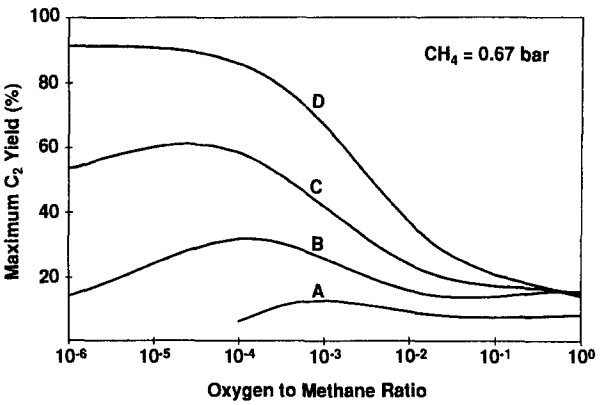

Fig. 4. Simulated effects of a fixed oxygen concentration on C_2 yields in a tubular membrane reactor. (1073 K, 67 kPa methane) (Curve A: homogeneous reactions, $N = 0$; curve B: heterogeneous–homogeneous reactions, $N = 1.0\ s^{-1}$, $n = 1$, $g = 0$; curve C: $N = 1.0\ s^{-1}$, $n = 0.5$, $g = 0$; curve D: $N = 1.0\,s^{-1}, n = 0, g = 0$.)

C_2 selectivity or yield improvements reported in ref. [25] cannot arise from the distribution of the oxygen reactant equally between two injection points.

Controlled introduction into oxidative coupling reactors can also be achieved by cyclic operation of reactors or by using oxygen-storing solids. In the Arco cyclic process, solids are transferred between oxygen-charging and methane conversion reactors [26,27]. The oxygen introduced in the first step is gradually released in the second stage by solid-state diffusion processes. Cycling of reactants between C_2 and CH_4–O_2 mixtures on packed beds containing Ce/Li/MgO catalysts, however, did not improve C_2 yields [28], not a surprising result because of the low oxygen storage capacity of these materials and of the use of high oxygen concentrations even in the methane conversion cycle. Low oxygen concentrations can also be achieved using raining solids reactors, where oxygen-containing solids decompose gradually and evolve O_2 as they fall through the interpellet voids within a packed-bed reactor.

3.4. MEMBRANE AND BACKMIXED REACTORS SYSTEMS

High-conversion backmixed or controlled-injection and membrane reactors can also maintain constant low oxygen concentrations, while continuously supplying the required oxygen reactants. High dispersion and rapid backmixing achieved in fluid-bed or stirred tanks reactors are ideally suited for oxidative coupling reactions at low oxygen concentrations [29,30]. In backmixed systems, reactor concentrations and exit concentrations are identical; therefore, methane and oxygen conversion levels, and the oxygen concentration at which oxidative coupling reactions proceed, can be controlled by varying reactor residence time and the level of oxygen depletion. Oxygen concentrations can also be controlled by supplying oxygen in a continuous manner along a plug-flow reactor with fast radial dispersion in order to achieve similar effects. This latter approach has been experimentally tested using oxygen-conducting solid state membranes [31–33].

Our simulations predict that low oxygen content in membrane reactors favor higher C_2 yields, but only at concentration levels (oxygen/methane $< 10^{-3}$) too low for efficient industrial practice (fig. 4). Homogeneous reactors (curve A) and bimodal reactors with first-order catalytic systems (curve B) benefit only slightly from low oxygen concentrations. Catalytic sites with weaker oxygen dependence (curve C, $n = 0.5$; curve D, $n = 0$) lead to significant C_2 yields (60–90%) at low oxygen concentrations. The results in fig. 4 were obtained using a tubular membrane reactor model. In this model, methane concentrations decrease along the axial reactor dimension as conversion proceeds but O_2 levels are maintained constant by a continuous supply through the reactor wall. In contrast with totally backmixed reactors, where concentrations of both CH_4 and O_2 remain constant throughout the reactor, our simulations describe a membrane reactor where only the O_2 reactant is "backmixed", i.e., evenly distributed throughout the reactor. The combination of sites with weak oxygen kinetic dependence and "oxygen-starved" backmixed or

membrane reactors can lead to C_2 yields as high as 90% in oxidative coupling of methane. Reactors at such low oxygen concentrations, however, must operate at extremely low space velocities and will require much larger reactor volumes and catalyst charges than conventional reactors because of the weak kinetic driving force for heterogeneous methyl radical generation (except for catalysts with zero-order oxygen kinetics).

Very low oxygen levels ultimately decrease C_2 yields because of the consequent decrease in methyl radical concentration (fig. 4). At these conditions, monomolecular reactions of methyl radicals with O_2 are favored over bimolecular methyl coupling steps; as a result, the benefits of heterogeneous radical generation sites are rapidly lost, except on reaction sites with zero-order oxygen kinetics.

3.5. TRANSPORT RESTRICTIONS WITHIN POROUS CATALYST PELLETS

The porous nature of catalytic pellets can introduce diffusional barriers that prevent the attainment of external concentrations throughout a pellet. This leads to lower reactant, and higher product, concentrations within pellets than in the interpellet reactor voids. Intrapellet transport restrictions often lead to inefficient use of catalytic sites because they lower reactant concentrations and the kinetic driving force for chemical reactions. Frequently, transport restrictions also enhance secondary reactions of reactive primary products, such as the conversion of ethane and ethylene to CO_x in oxidative methane coupling. In oxidative coupling reactions, however, oxygen becomes the diffusion-limited reactant and intrapellet oxygen concentration gradients are sharper than for methane. Therefore, low oxygen concentrations, which can increase C_2 selectivity and yield, can be achieved by intrapellet transport restrictions that limit the rate of O_2 arrival at catalytic sites.

The severity of diffusional limitations is typically characterized by a combination of reactive and structural properties called the Thiele modulus,

$$\Phi_i^2 = \emptyset_i\left(R_0 \varepsilon \Theta / r_p\right) = \emptyset_i \chi \,. \tag{4}$$

This dimensionless parameter reflects the ratio of reaction to diffusion rate for each chemical species. It is obtained from a rigorous dimensional analysis of the intrapellet reaction–diffusion equations discussed in section 2.3 and described in detail elsewhere [5]. In eq. (4), we have conveniently separated the reactivity properties ($\emptyset_i$) from the structural properties of the porous material (R_0: pellet radius, ε: porosity, Θ: site density, r_p: pore radius). The latter are more readily controlled by the catalyst designer, whereas the former tend to reflect intrinsic chemical properties of the catalytic material and of the reacting molecule. Diffusional restrictions become more severe as we increase the Thiele modulus by an appropriate change in any of the structural (χ) or reactive ($\emptyset_i$) properties appearing in eq. (4). Here, we have chosen the pellet radius as the experimental variable in order to illustrate the effect of intrapellet oxygen sieving on C_2 selectivity (fig. 5).

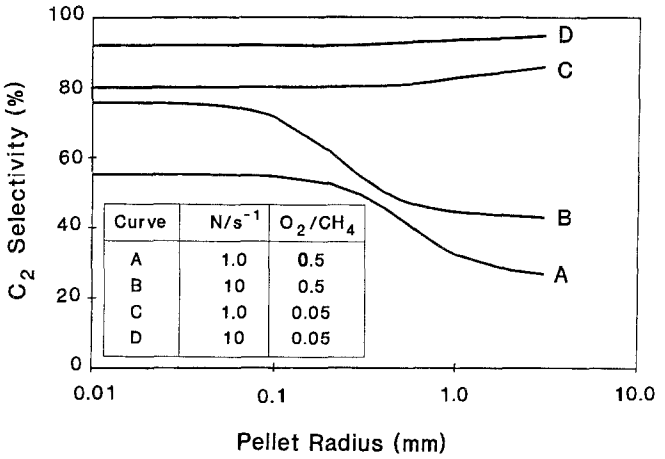

Fig. 5. Simulated effect of pellet radius on C_2 selectivity (1073 K, 67 kPa methane, 10% methane conversion; kinetic properties: $n = 0.5, g = 4$.)

The C_2 selectivity (at 10% methane conversion) is not affected by pellet radius for small pellets (<0.1 mm, curve A, fig. 5). Such pellets are not limited by transport rates; therefore, intrapellet reactant and product concentrations remain identical to those within interpellet reactor voids. Pellets larger than 0.1 mm introduce intrapellet concentration gradients and a decrease in C_2 selectivity. The onset of diffusional restrictions occurs on smaller pellets for catalysts with higher activity (curves A and B, fig. 5). Therefore, the yield improvements anticipated on high activity materials (fig. 2) can quickly disappear in practice because of the ensuing transport restrictions within high activity catalyst pellets of usual diameter.

The beneficial effects of oxygen-sieving using intrapellet oxygen transport restrictions are not realized at high oxygen/methane ratios (curves A and B, fig. 5). In effect, the intrapellet gradients that develop at the high oxygen/methane feed ratios (0.5) of these simulations retain intrapellet concentrations in a range where they influence C_2 selectivities only slightly (fig. 4). As a result, the intrapellet retention of C_2 molecules and their secondary oxidation to CO_x offset any potential benefits of low intrapellet oxygen concentrations and C_2 selectivities actually decrease with increasing pellet size.

Beneficial oxygen-sieving effects can be achieved, however, by lowering oxygen/methane ratios within interpellet reactor voids. The, concentration gradients within transport-limited pellets decrease oxygen levels to those required to increase C_2 selectivities (fig. 4). For example, oxygen/methane ratios of 0.05 prevent the marked decrease in C_2 selectivity with increasing pellet size observed at higher oxygen concentrations. At these conditions, C_2 selectivity increases slightly as diffusional restrictions worsen (curves C and D, fig. 5).

Follmer et al. [34] reported that larger pellets of NaOH/CaO catalysts are more selective than smaller pellets. Their experiments were carried out with feeds

of low oxygen/methane ratio (0.1), where our simulations predict only a slight increase in C_2 selectivity with increasing pellet size. Their selectivity improvements are much greater than our model predicts. Their catalysts, however, were not very selective for C_2 formation even at low conversions, suggesting the presence of catalytic oxidation sites. The selectivity improvements that they report may well arise from the additional inhibition of catalytic oxidation pathways at the low intrapellet oxygen levels within transport-limited catalysts. Their proposed reaction–transport model neglects homogeneous reaction steps and describes oxidative coupling using two empirical kinetic steps, one for methane conversion to C_2 and higher hydrocarbons and one for methane oxidation to CO and CO_2 [34].

The reaction–transport model described by Santamaria et al. [35] for oxidative coupling catalyst pellets was also restricted to a very simplified empirical kinetic model. Their kinetic model lumps homogeneous–heterogeneous reactions into three groups: coupling of methane to C_2 products and full oxidation of methane and C_2 to CO_x. Neither of the two available models [34,35] includes detailed kinetic descriptions or examines the design of catalysts with desired textural or chemical properties for improved C_2 yields, a significant distinction from the approach in our study.

Low oxygen concentrations permit the use of larger pellets and more active sites by lowering the heterogeneous activation rate and the volumetric productivity of each pellet (cf. curves B and D, fig. 5). Therefore, C_2 product concentration gradients become less steep than on similar pellets used at higher oxygen/methane ratios. At low oxygen levels, intrapellet oxygen concentrations are sufficiently low to inhibit the secondary oxidation of desired C_2 products to CO_x. Our simulations suggest that the low oxygen concentrations imposed by distributed oxygen reactors are essential in order to avoid the damaging effects of intrapellet transport restrictions on very active catalysts and to exploit the limited oxygen-sieving benefits of diffusion-limited pellets in oxidative coupling reactions.

3.6. OTHER CONSEQUENCES OF POROUS CATALYTIC PELLETS

Reaction and transport processes can also lead to concentration gradients of very reactive species (e.g. $\cdot CH_3$, $\cdot C_2H_5$, $\cdot OH$, ...) across a pore diameter, a much smaller characteristic length scale than the radial intrapellet gradients considered in section 3.5. The corresponding Thiele modulus would then include rate constants for the much faster reactions of very reactive free radicals but also a much smaller characteristic diffusion distance. A detailed description of these processes is beyond the scope of our paper but we comment here on the qualitative consequences of reaction–transport coupling occurring within the scale of a pore diameter, a critical aspect of oxidative coupling recently discussed by McCarty [36].

Bimodal oxidative coupling schemes require that reactants collide repeatedly with the solid pore walls and form methyl radicals. They also require that the ratio

of solid surface to available void volume be large to ensure a significant heterogeneous contribution to methyl formation rates. Thus, we require small pores, which also avoid radial concentration gradients and ensure high methyl radical concentrations. Yet, methyl radicals must collide in the gas phase, preferably before they readsorb on a surface site and oxidize further to CO_x products. This requires that the characteristic times for reactive collisions be short compared with the diffusion times required for travel across a pore diameter. Thus, large pores and high gas phase concentrations favor coupling steps, but these requirements conflict with those required for effective heterogeneous activation steps.

This qualitative treatment suggests that intermediate values of pore diameter, surface area, and reactant pressures are needed to balance these competing requirements. This suggests that oxidative coupling reactions benefit when gas phase diffusion occurs by a combination of molecule–surface (Knudsen diffusion) and molecule–molecule (bulk diffusion) collisions. This transition diffusion regime offers an appropriate compromise between required gas phase and surface collisions of methane reactants and of gas phase collisions of free radical intermediates.

In general, low surface areas are required to prevent secondary reactions in catalytic sequences involving reactive products, but overall reaction rates then become very slow, leading to optimum yields at intermediate values of surface area and pore size. In oxidative coupling, selectivity also ultimately decreases with decreasing surface area because heterogeneous radical formation rates no longer maintain high steady-state concentrations of methyl radicals required in coupling steps [37]. Similar trends have been recently reported with varying site density for Pb/MgO catalysts [38], where the selectivity reaches a maximum at intermediate values of site density, controlled by varying the PbO loading.

4. Conclusions

Our work describes the use of detailed kinetic–transport models of bimodal homogeneous–heterogeneous chemical reactions. These models guide the optimal design of catalytic pellets and reactors for our chosen example: the oxidative coupling of methane. They contain a homogeneous reaction network and a surface reaction model described by kinetic and structural catalyst design parameters. Simulations using these models suggest several routes for improvements in currently attainable C_2 yields, specifically staged injection and membrane reactors using catalysts with high densities of sites and low order oxygen kinetics. Our simulations also confirm in a rigorous manner the previously suggested need for more active and selective catalysts in oxidative coupling of methane. They offer a sound modeling framework for understanding some of the conflicting literature reports on the effects of staged oxygen injection and of diffusion-limited pellets on C_2 yields and selectivities.

References

[1] D. Gray and G. Tomlinson, Report SAND-88-7110, Sandia National Laboratories (1988).
[2] J.H. Lunsford, Langmuir 5 (1989) 12.
[3] J.S. Lee and S.T. Oyama, Catal Rev.-Sci. Eng. 30 (1988) 249.
[4] Y. Amenomiya, V.I. Birss, M. Goladzinowski, J. Galuszka and A.R. Sanger, Catal. Rev.-Sci. Eng. 32 (1990) 163.
[5] S.C. Reyes, E. Iglesia and C.P. Kelkar, Chem. Eng. Sci., accepted.
[6] S.C. Reyes, E. Iglesia and C.P. Kelkar, Abstracts 12th North American Meeting of the Catalysis Society, Lexington, KY, 1991.
[7] S.C. Reyes and E. Iglesia, J. Catal. 129 (1991) 457.
[8] G.B. Skinner, A. Lifshitz, K. Scheller and A. Burcat, J. Chem. Phys. 56 (1984) 3853.
[9] J. Warnatz, in: *Combustion Chemistry*, ed. W.C. Gardiner (Springer, Berlin, 1990).
[10] H. Zanthoff and M. Baerns, Ind. Eng. Chem. Res. 29 (1990) 2.
[11] J.C. Mackie, J.G. Smith, P.F. Nelson and R.J. Tyler, Energy and Fuels 4 (1990) 277.
[12] G.S. Bahn, Pyrodynamics 2 (1965) 315.
[13] W. Tsang and R.F. Hampson, J. Phys. Chem. Ref. Data 15 (1986) 1087.
[14] J.A. Labinger and K.C. Ott, J. Phys. Chem. 91 (1987) 2682.
[15] J.G. McCarty, A.b. McEwen and M.A. Quinlan, in: *New Developments in Selective Oxidation*, eds. G. Centi and F. Trifiro (Elsevier, Amsterdam, 1990) p. 405.
[16] T.A. Garibyan and L.Ya. Margolis, Catal. Rev.-Sci. Eng. 31 (1989/1990) 355.
[17] J.W.M.H. Geerts, Q. Chen, J.M.N. van Kasteren and K. van der Wiele, Catal. Today 6 (1990) 519.
[18] Y. Feng, J. Niiranen and D. Gutman, J. Phys. Chem. 95 (1991) 6558.
[19] Y. Feng, J. Niiranen and D. Gutman, J. Phys. Chem. 95 (1991) 6564.
[20] G.S. Lane and E.E. Wolf, J. Catal. 113 (1988) 144.
[21] M.W. Droege, L.M. Hiar, W.J. Pitz and C.K. Westbrook, SPE 19081 (1989) 247.
[22] L.M. Aparicio, S.A. Rossini, D.M. Sanfilippo, J.E. Rekoske, A.A. Trevino and J.A. Dumesic, Ind. Eng. Chem. Res. 30 (1991) 2114.
[23] V.R. Choudhary, S.T. Chaudhari, A.M. Rajput and V.H. Rane, J. Chem. Soc. Chem. Commun. (1989) 1526.
[24] J. Santamaria, M. Menendez, J.A. Peña and J.I. Barahona, Catal. Today 13 (1992) 353.
[25] K.J. Smith and J.Z. Galuszka, United States Patent 5,132,482 (1992), assigned to Alberta Research Council.
[26] C.A. Jones, J.J. Leonard and J.A. Sofranko, Energy and Fuels 1 (1987) 12.
[27] A. Gaffney, C.A. Jones, J.J. Leonard and J.A. Sofranko, in: *Catalysis*, ed. J.W. Ward (Elsevier, Amsterdam, 1988).
[28] Y. Mortazavi, R.R. Hudgins and P.L. Silveston, in: *Progress in Catalysis*, eds. K.J. Smith and E.C. Sanford (Elsevier, Amsterdam, 1992) p. 119.
[29] J.H. Edwards, K.T. Do and R.J. Tyler, Catal. Today 6 (1990) 435.
[30] L. Mleczko, R. Andorf and M. Baerns, Chem. Eng. Technol. 14 (1991) 325.
[31] D. Eng and M. Stoukides, in: *Proc. 9th Int. Congr. on Catalysis*, Vol. 2, eds. M.J. Phillips and M. Ternan (The Chemical Society of Canada, Ottawa, 1988) p. 974.
[32] K. Omata, S. Hashimoto, H. Tominaga and K. Fujimoto, Appl. Catal. 52 (1989) L1.
[33] N. Mouaddib, K.R. Thampi, A.J. McEvoy, J. Kiwi and M. Gratzel, Catal. Lett. 5 (1990) 285.
[34] G. Follmer, L. Lehmann and M. Baerns, Catal. Today 4 (1989) 323.
[35] J.M. Santamaria, E.E. Miro and E.E. Wolf, Ind. Eng. Chem. Res. 30 (1991) 1157.
[36] J.G. McCarty, American Chemical Society, Div. Petr. Chem. Preprint 36 (1991) 142.
[37] N.I. Il'chenko, L.N. Raevskaya, A.I. Bostan and G.I. Golodets, Kinet. Katal. 32 (1991) 873.
[38] S.K. Agarwal, R.A. Migone and G.J. Marcelin, J. Catal. 121 (1990) 110.